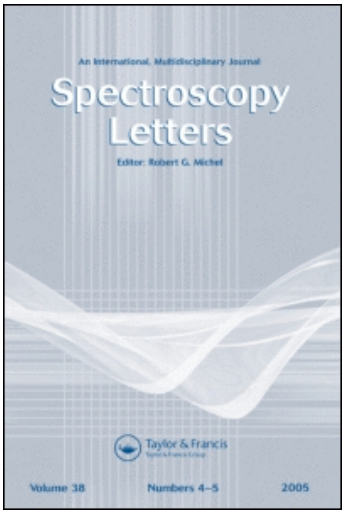

Spectroscopy Letters
Publication details, including instructions for authors and subscription information:
http://www.informaworld.com/smpp/title~content=t713597299

Analysis of hyperfine structure of Rare-Earth Ions in Single Crystals by Electron Paramagnetic Resonance Spectroscopy

Olivier Guillot-Noël[a]; Philippe Goldner[a]; Yann Le Du[a]
[a] Laboratoire de Chimie de la Matière Condensée de Paris (LCMCP), Paris, France

To cite this Article Guillot-Noël, Olivier , Goldner, Philippe and Du, Yann Le(2007) 'Analysis of hyperfine structure of Rare-Earth Ions in Single Crystals by Electron Paramagnetic Resonance Spectroscopy', Spectroscopy Letters, 40: 2, 247 — 257
To link to this Article: DOI: 10.1080/00387010701247365
URL: http://dx.doi.org/10.1080/00387010701247365

Spectroscopy Letters, 40: 247–257, 2007

ISSN 0038-7010 print/1532-2289 online
DOI: 10.1080/00387010701247365

Analysis of hyperfine structure of Rare-Earth Ions in Single Crystals by Electron Paramagnetic Resonance Spectroscopy

Olivier Guillot-Noël, Philippe Goldner, and Yann Le Du
Laboratoire de Chimie de la Matière Condensée de Paris (LCMCP), Paris, France

Abstract: Electron paramagnetic spectroscopy of rare-earth ions in single crystals is an interesting tool to analyze the hyperfine structure of the ground state of the rare-earth. This can be useful for coherent spectroscopy and quantum information applications where the hyperfine structure of the electronic levels is used. Moreover, in some cases, the electron paramagnetic resonance hyperfine structure of interacting rare-earth ions allows us to retrieve the isotropic exchange interaction between the two interacting ions. We illustrate these points with the hyperfine structure of Yb^{3+} ions in vanadate crystals, the hyperfine structure of Er^{3+} ions in Y_2SiO_5, and the hyperfine structure of Yb^{3+} pairs in $CsCdBr_3$.

Keywords: Electron paramagnetic resonance, hyperfine structure, pair interaction, rare-earth ions

INTRODUCTION

Electron paramagnetic spectroscopy of rare-earth ions in single crystals is an interesting spectroscopy to analyze the hyperfine structure of the ground state of the rare-earth. Rare-earth hyperfine structure is useful in coherent

Received 1 June 2006, Accepted 24 August 2006
The authors were invited to contribute this paper to a special issue of the journal entitled "Spectroscopy of Lanthanide Materials." This special issue was organized by Professor Peter Tanner, City University of Hong Kong, Kowloon.
Address correspondence to Olivier Guillot-Noël, Laboratoire de Chimie de la Matière Condensée de Paris (LCMCP), ENSCP, CNRS-UMR 7574, 11 rue Pierre et Marie Curie, F-75231 Paris, France. E-mail: olivier-guillotn@enscp.fr

spectroscopy[1] and related quantum information applications. As the hyperfine splittings (few hundred megahertz) even at low temperature are usually smaller than the optical inhomogeneous linewidth (few gigahertz), they can only be determined by hole burning spectroscopy, but only where the hole lifetime is long enough. Very often, if the rare-earth ion has high values of nuclear spins, the hole burning spectra are difficult to analyze and the hyperfine structure remains unknown.

Moreover, optical spectra of rare-earth (RE) ions in crystals often exhibit extra features that are difficult to analyze precisely. For example, extra transitions can be due to interacting ions that can have important effects on luminescent properties.

Electron paramagnetic resonance (EPR) spectroscopy of Kramers' ions can be very useful in solving these problems; that is, the hyperfine structure analysis and rare earth-rare earth interactions. Although usually limited to the ground-state crystal field level, this technique has two main advantages over its optical counterpart. First, the inhomogeneous linewidth of the Zeeman transitions in RE ions is approximately three orders of magnitude smaller than those observed in the optical domain. This allows one to observe very clearly splittings due to the hyperfine structure. Moreover, by rotating a single crystal in the magnetic field, precise information on the site symmetry (including ground-state irreducible representation) and also on the orientation and distance between interacting ions can be easily retrieved. EPR spectroscopy is also very convenient to determine hyperfine structures in complicated cases where $\tilde{g}$, $\tilde{A}$ matrices are not coaxial or in the case of magnetically inequivalent RE sites.

The aim of this paper is to show how with the use of EPR spectroscopy, we can determine the hyperfine structure of the ground state of Kramers' ions. We prove this with results obtained by our group: i) the hyperfine structure of Yb^{3+} ions in vanadate crystals,[2] and of Er^{3+} ions in Y_2SiO_5; ii) the hyperfine structure of Yb^{3+} in $CsCdBr_3$ to probe ion–ion interactions.[3,4]

HYPERFINE STRUCTURE OF GROUND-STATE KRAMERS' IONS

Free Kramers' ions have a $4f^n$ configuration with odd value of n with a $^{2S+1}L_J$ ground state with J half-integer. S, L, J are the spin, orbital and total momenta, respectively. For example, free Yb^{3+} ion has a $4f^{13}$ configuration with a $^2F_{7/2}$ ground state; free Er^{3+} ion has a $4f^{11}$ configuration with a $^4I_{15/2}$ ground state. In a crystal field of low symmetry, the $^{2S+1}L_J$ manifold splits into $(2J+1)/2$ Kramer's doublets with $|M_J| = J, J-1,\ldots,1/2$, M_J being the z-component of J. Only the lowest doublet is populated at liquid helium temperature, therefore the Kramers' ions from an EPR point of view can be described by a fictitious spin $S = 1/2$. Very often, Kramers' ions have isotopes with zero and non-zero nuclear spins I. In this case, the EPR spectrum is expected to be composed of a central line due to isotopes with zero nuclear spins and a hyperfine pattern

composed of at least $2I + 1$ lines for each different isotope with non-zero nuclear spins and relative intensities proportional to their natural abundances.

EPR measurements were performed with a X-band Bruker Elexsys E 500 spectrometer (Bruker Biospin, Karlsruhe) equipped with an Oxford Instrument (UK) variable temperature device. The crystals were mounted on a small Perspex sample holder to allow their orientation with respect to the magnetic field. Angular variations were obtained by rotating the crystal by steps of 10 degrees.

Ytterbium has five even isotopes, ^{168}Yb, ^{170}Yb, ^{172}Yb, ^{174}Yb, and ^{176}Yb, with nuclear spins $I = 0$ and a total natural abundance of 69.58%, and two odd isotopes, ^{171}Yb with nuclear spin $I = 1/2$ (natural abundance 14.3%) and ^{173}Yb with nuclear spin $I = 5/2$ (natural abundance 16.12%). The EPR spectrum of Yb^{3+} ions is expected to be composed of an intense central line due to even isotopes and a hyperfine pattern composed of two sets of 2 and 6 lines for the two odd isotopes. Figure 1 shows the experimental and simulated EPR spectra at 6.5 K of 1% Yb-doped $LuVO_4$ single crystals with the magnetic field parallel to the c axis.[2] $LuVO_4$ crystallizes in the zircon type structure and belongs to the tetragonal $I4_1/amd$ space group. Yb^{3+} ions substitute eightfold coordinated Y^{3+} ions, forming $[YO_8]$ bisdisphenoids with D_{2d} point site symmetry. The angular variations of the Yb^{3+} EPR signal reflect the axial symmetry of the ytterbium site, which can be described by the following spin-Hamiltonian:

$$H = g_{//}\beta_e B_z S_z + g_{\perp}\beta_e (B_x S_x + B_y S_y) + A_{//} I_z S_z + A_{\perp}(I_x S_x + I_y S_y), \quad (1)$$

with $S = 1/2$ and $I = 0$, $1/2$ or $5/2$. β_e is the electronic Bohr magneton. No quadrupole interaction is included because we do not see any effect of this interaction in our EPR spectra. The spin-Hamiltonian g-factor components,

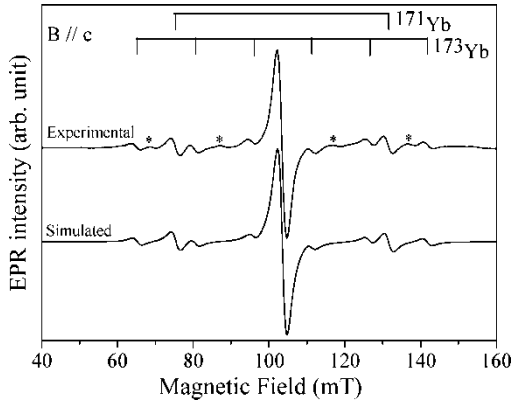

Figure 1. Experimental and simulated EPR spectra at 6.5 K of ions in $LuVO_4$:1% Yb^{3+} single crystals with the magnetic field parallel to the c axis. The stars indicate lines that can be due to forbidden transitions.

$g_{//}$ and $g_{\perp}$, are determined by fitting the experimental angular variations of the central line. The principal axes of the g-factor are found to be parallel to the crystallographic axes and the principal g-values are $|g_{x,y} = g_{\perp}| = 0.59(7)$ and $|g_z = g_{//}| = 6.464(9)$. The hyperfine interaction exhibits the same axial symmetry with the principal $A_{//}$ component parallel to the c axis. The hyperfine structure is clearly seen when the magnetic field is parallel to the c axis. However, when the magnetic field rotates from the c axis to the direction of the (001) plane, the lines broaden and the hyperfine pattern is not seen anymore. It is only possible to determine the $A_{//}$ component by fitting the experimental spectrum with the magnetic field parallel to the c axis by using Eq. (1). We obtain $|A_{//}^{171}| = 5100$ and $|A_{//}^{173}| = 1390$ MHz. As we can neglect the J-mixing between the $^2F_{7/2}$ ground manifold and the $^2F_{5/2}$ excited multiplet, we have the following relationship between the spin-Hamiltonian parameters:[5]

$$\frac{g_{//}}{g_{\perp}} = \frac{A_{//}}{A_{\perp}}. \tag{2}$$

From Eq. (2), we deduce the perpendicular component of the hyperfine tensor: $|A_{\perp}^{171}| = 465$ and $|A_{\perp}^{173}| = 127$ MHz.

The previous study is simple because the point site symmetry of the rare-earth is axial in $LuVO_4$, which implies that the principal axes of the g-factor and of the hyperfine interaction are coincident. Moreover, the quadrupole interaction can be neglected by the determination of the hyperfine parameters from the position of the allowed hyperfine transitions.

A more complex hyperfine energy level structure is found when the point site symmetry is very low; as in the case of Er^{3+} ions in Y_2SiO_5 single crystals

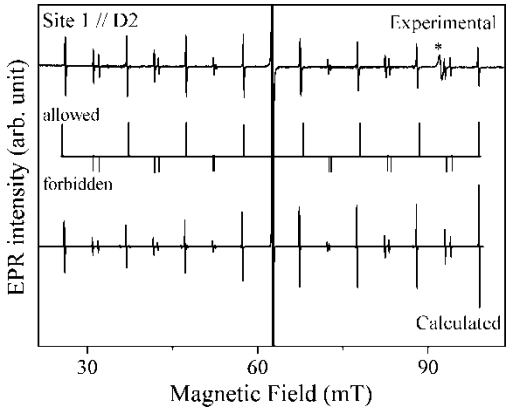

Figure 2. Experimental and simulated EPR spectra at 8 K of Er^{3+} ions in site 1 in Y_2SiO_5 single crystals with the magnetic field parallel to the D_2 axis. The star indicates a line that is due to site 2. The sample is doped with 0.005% of Er^{3+} ions.

(Fig. 2). Erbium has five even isotopes, ^{162}Er, ^{164}Er, ^{166}Er, ^{168}Er, and ^{170}Er, with nuclear spins $I = 0$ and a total natural abundance of 77.05%, and one odd isotope, ^{167}Er, with nuclear spin $I = 7/2$ (natural abundance 22.95%). The EPR spectrum of Er^{3+} ions is expected to be composed of an intense central line due to even isotopes and a hyperfine pattern composed of 8 lines for the odd isotope. Y_2SiO_5 has a monoclinic structure with $C2/c$ space group. Er^{3+} ions lie on two crystallographic sites with low symmetry C_1 with seven and six oxygen neighbors. In the following analysis, we are only interested in site 1 characterized in Ref. 6 by the 1536.48-nm vacuum wavelength for the lowest $^4I_{15/2}$ to $^4I_{13/2}$ transitions. Very low site symmetries will induce a strong mixing between the different M_I projections of the nuclear spin I, and allowed and forbidden hyperfine transitions will appear in the EPR spectrum (Fig. 2). The following spin-Hamiltonian describes the EPR spectra for the ^{167}Er isotope:

$$H = \beta_e S \cdot \tilde{g} \cdot B + S \cdot \tilde{A} \cdot I + I \cdot \tilde{Q} \cdot I - \beta_n g_n I \cdot B, \tag{3}$$

where β_n is the nuclear Bohr magneton, g_n is the nuclear g-factor, $\tilde{g}$ is the g-factor matrix, and $\tilde{A}$ and $\tilde{Q}$ are the hyperfine and quadrupole matrices, respectively. $\tilde{Q}$ is a traceless matrix. In a site of C_1 symmetry, the principal axes of each interaction are not coincident. The determination of $\tilde{g}$, $\tilde{A}$, and $\tilde{Q}$ matrices with respect to a reference axis set is obtained from the angular variations of the experimental EPR spectra in three orthogonal crystal planes. In this work, the three reference axes are the optical extinction axes D1, D2, and b defined in Ref. 6. The following matrices representing the $\tilde{g}$, $\tilde{A}$, and $\tilde{Q}$ interactions in the (D1, D2, b) axis system can be generated:

$$\tilde{g} = \begin{bmatrix} g_{\mathrm{D1D1}} & g_{\mathrm{D1D2}} & g_{\mathrm{D1b}} \\ g_{\mathrm{D1D2}} & g_{\mathrm{D2D2}} & g_{\mathrm{D2b}} \\ g_{\mathrm{D1b}} & g_{\mathrm{D2b}} & g_{\mathrm{bb}} \end{bmatrix}_{(\mathrm{D1D2b})} \tag{4}$$

$$\tilde{A} = \begin{bmatrix} A_{\mathrm{D1D1}} & A_{\mathrm{D1D2}} & A_{\mathrm{D1b}} \\ A_{\mathrm{D1D2}} & A_{\mathrm{D2D2}} & A_{\mathrm{D2b}} \\ A_{\mathrm{D1b}} & A_{\mathrm{D2b}} & A_{\mathrm{bb}} \end{bmatrix}_{(\mathrm{D1D2b})} \tag{5}$$

$$\tilde{Q} = \begin{bmatrix} Q_{\mathrm{D1D1}} & Q_{\mathrm{D1D2}} & Q_{\mathrm{D1b}} \\ Q_{\mathrm{D1D2}} & Q_{\mathrm{D2D2}} & Q_{\mathrm{D2b}} \\ Q_{\mathrm{D1b}} & Q_{\mathrm{D2b}} & -(Q_{\mathrm{D1D1}} + Q_{\mathrm{D2D2}}) \end{bmatrix}_{(\mathrm{D1D2b})} \tag{6}$$

In the general case, $\tilde{g}$ and $\tilde{A}$ are asymmetric, however such an effect could not be seen in our spectra. In this reference axis set, we thus have to determine 17 spin-Hamiltonian parameters. The 6 g-factor matrix elements are obtained from the angular study of the central EPR line of the even isotopes. The other 11 parameters are obtained from angular variations of the allowed and forbidden hyperfine transitions. The angular variations were obtained by rotating the crystals by steps of 10

degrees around reference axes with a 1 degree estimated accuracy for crystal orientation. Figure 2 shows the experimental and simulated EPR spectra at 8 K of an 0.005% Er^{3+}-doped Y_2SiO_5 single crystal with the magnetic field parallel to the D_2 axis. The EPR spectrum corresponds with Er^{3+} ions in site 1. The star indicates a line that is due to site 2. The spectrum is composed of eight allowed hyperfine transitions. Between each allowed transition, pairs of forbidden transitions are observed. Those transitions are due to second-order effects of the hyperfine interaction and to the quadrupole interaction. The splitting between each pair of forbidden transitions is only due to the quadrupole interaction. As the intensities of the forbidden lines are of the same order of magnitude as the allowed transitions, the quadrupole interaction cannot be treated as a perturbation of the hyperfine interaction. The nuclear Zeeman interaction [last term of Eq. (3)] does not influence the position of the allowed and forbidden transitions but it does influence their intensities. To determine the 11 spin-Hamiltonian parameters, we perform a complete diagonalization of the Hamiltonian of Eq. (3). The calculated positions are compared with the experimental ones and the different parameters are determined by minimizing the RMS_{norm} parameter defined by:

$$RMS_{norm} = \left[\frac{1}{N-11}\sum_{i=1}^{N}\left(\frac{B_i^{\exp} - B_i^{calc}}{err_i}\right)\right]^{1/2}, \tag{7}$$

where $B_i^{\exp}$ and B_i^{calc} are the experimental and calculated magnetic field positions. To get a quantitative measure of the goodness of fit, errors (err_i) have to be taken into account. For each experimental position, the errors are determined by assuming a 1 degree accuracy for crystal orientations. The sum runs from 1 to N where N is the number of experimental data points. For the hyperfine and quadrupole interactions, 1109 experimental positions are used to optimize the 11 parameters. The subscript "norm" emphasizes the use of normalized experimental data (i.e., by taking explicitly into account their errors). Fitting normalized data is necessary to ensure that positions measured with the same accuracy have the same weight in the fit. A $RMS_{norm} = 0.93$ is obtained giving the following matrices for the different interactions:

$$\tilde{g} = \begin{bmatrix} 2.92 & -3.08 & -3.68 \\ -3.08 & 8.19 & 5.96 \\ -3.68 & 5.96 & 5.52 \end{bmatrix}_{\text{(D1D2b)}} \tag{8}$$

$$\tilde{A} = \begin{bmatrix} 69.35 & -580.73 & -248.83 \\ -580.73 & 696.30 & 682.49 \\ -248.83 & 682.49 & 495.54 \end{bmatrix}_{\text{(D1D2b)}} \tag{9}$$

$$\tilde{Q} = \begin{bmatrix} 21.40 & -8.18 & -15.27 \\ -8.18 & 3.79 & 0.60 \\ -15.27 & 0.60 & -25.20 \end{bmatrix}_{\text{(D1D2b)}}, \tag{10}$$

with $\tilde{A}$ and $\tilde{Q}$ given in MHz. Some matrix elements of the quadrupole interaction are of the same order of magnitude as the hyperfine interaction. This confirms that a perturbative treatment of the spin-Hamiltonian was not appropriate in this case.

To test the validity of these parameters, we can calculate the EPR spectrum of Er^{3+} ions for a very general orientation of the static magnetic field and compare this calculated spectrum to the experimental one. Figure 2 gathers the experimental and the calculated spectrum for the magnetic field parallel to the D2 axis. There is a good agreement between these two spectra. The positions and intensities of the different allowed and forbidden lines are well reconstructed.

This last case demonstrates that even in very low symmetry site, EPR spectroscopy allows one to retrieve precisely all the magnetic parameters of the hyperfine structure of the ground state. The hyperfine structure can then be calculated for an arbitrary orientation and intensity of the magnetic field and in particular at zero field. This is the case usually encountered in optical spectroscopy. Having determined the ground-state hyperfine splitting by EPR, hole burning spectroscopy can then be used to retrieve the excited-state hyperfine structure.

HYPERFINE STRUCTURE OF INTERACTING RARE-EARTH IONS

Research on materials doped with rare-earth ion pairs and clusters is of fundamental interest for several applications like intrinsic optical bistability.[7] In the field of quantum information and quantum computing, a scheme for generating interacting quantum bits in rare-earth-ion–doped crystals has been proposed in Ref. 8. Coupling between rare-earth ions is necessary to perform controlled logic. Two important interactions can be measured from an EPR spectrum of pairs: the dipole–dipole magnetic interaction and the isotropic exchange interaction.[4] From the dipole–dipole interaction, the rare-earth pair orientation in the host can be determined and the interionic distances between the two ions can be calculated. Two cases have to be considered: i) pairs of similar ions characterized by the same ground state g value and ii) pairs of dissimilar ions characterized by different ground state g values where the ions in the pair can be different or identical with slightly different crystal fields. In the case of identical ions with the same g values, the EPR spectrum of isotopes with no nuclear spin consists of a doublet of lines separated by the magnetic dipole–dipole interaction. The isotropic exchange interaction cannot be measured by EPR in this case. However, if the interacting rare-earth ions have isotopes with nuclear spins, the hyperfine structure allows us to retrieve the isotropic exchange interaction.[3] The Yb:$CsCdBr_3$ host corresponds with the case of identical ions with a very

small isotropic exchange interaction. A well-known feature of $CsCdBr_3$ is that rare-earth ions such as Yb^{3+}, even at low doping concentration, enter nearly exclusively as charge compensated ion–pair centers in the Cd^{2+} lattice position. The main rare-earth center is a symmetric in-chain Yb^{3+}–V_{Cd}–Yb^{3+} pair complex, where V_{Cd} means Cd^{2+} vacancy, oriented along the c axis. The EPR signal of ytterbium ions in $CsCdBr_3$ is shown in Figure 3 for the external magnetic field parallel to the pair axis (*c* axis). The complexity of the spectra is due to the fact that Yb^{3+} ions has one even isotope of natural abundance 69% and two odd isotopes which are responsible for the hyperfine structure. All the spectral features can be accurately described by assigning the resonance lines to the symmetric pairs of identical ions of the type ^{even}Yb–V_{Cd}–^{even}Yb, ^{171}Yb–V_{Cd}–^{even}Yb, and ^{173}Yb–V_{Cd}–^{even}Yb.

The spin-Hamiltonian for a pair of identical interacting ions 1 and 2 can be written as:

$$H_{pair} = H_1 + H_2 + H_{int}. \tag{11}$$

As isolated ytterbium ions substitute Cd^{2+} ions in an axial site of C_{3v} symmetry, H_1 and H_2 are of the form of Eq. (1). The interaction term H_{int} is

$$H_{int} = -2JS_1 \cdot S_2 + \frac{\beta^2}{R^3}\left[-2g_{//}^2 S_{1z} S_{2z} + \frac{g_\perp^2}{2}(S_{1+}S_{2-} + S_{1-}S_{2+})\right]. \tag{12}$$

The first and the second terms in Eq. (12) are the isotropic exchange and anisotropic magnetic dipolar contribution, respectively. J is the isotropic exchange interaction, R is the rare earth–rare earth distance, and S_1 and S_2 are the effective spins of the lowest ground-state Kramers' doublet of the two ions. When there is no nuclear spin ($I = 0$) and the external magnetic

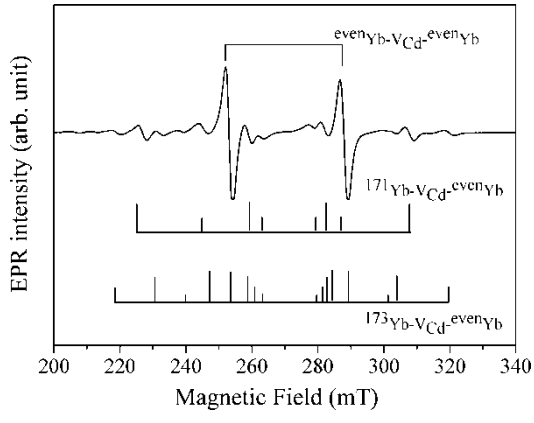

Figure 3. Experimental EPR spectrum of $CsCdBr_3$:1.3% Yb^{3+} at 7 K with the external magnetic field parallel to the crystallographic *c* axis. The stick diagram represents the calculated spectrum.

field is parallel to the pair axis (z axis), the eigenvalues and eigenvectors for H_{pair} are

$$E_1 = -g_{//}\beta B - \frac{J}{2} - \mathrm{D}_1 \quad |\varphi_1\rangle = |M_{S1} = -1/2, M_{S2} = -1/2\rangle$$
$$E_2 = \frac{3J}{2} + \mathrm{D}_2 \quad |\varphi_2\rangle = \frac{1}{\sqrt{2}}(|1/2, -1/2\rangle - |-1/2, +1/2\rangle)$$
$$E_3 = -\frac{J}{2} + \mathrm{D}_3 \quad |\varphi_3\rangle = \frac{1}{\sqrt{2}}(|1/2, -1/2\rangle + |-1/2, +1/2\rangle)$$
$$E_4 = g_{//}\beta B - \frac{J}{2} - \mathrm{D}_1 \quad |\varphi_4\rangle = |1/2, 1/2\rangle, \tag{13}$$

with

$$\mathrm{D}_1 = \frac{\beta^2}{2R^3} g_{//}^2, \mathrm{D}_2 = \frac{\beta^2}{2R^3}\left(g_{//}^2 - g_{\perp}^2\right), \mathrm{D}_3 = \frac{\beta^2}{2R^3}\left(g_{//}^2 + g_{\perp}^2\right).$$

The isotropic exchange interaction term splits the fourfold degenerate pair ground state $\{|\varphi_1\rangle, |\varphi_2\rangle, |\varphi_3\rangle, |\varphi_4\rangle\}$ into a singlet $|\varphi_2\rangle$ at energy $3J/2$ and into a triplet $\{|\varphi_1\rangle, |\varphi_3\rangle, |\varphi_4\rangle\}$ at energy $-J/2$. The dipolar interaction and the Zeeman term shift the singlet state $|\varphi_2\rangle$ by $+\mathrm{D}_2$ and split the triplet state into three singlet states $|\varphi_1\rangle$ at energy $-g_{//}\beta B - J/2 - \mathrm{D}_1$, $|\varphi_3\rangle$ at energy $-J/2 + \mathrm{D}_3$, and $|\varphi_4\rangle$ at energy $g_{//}\beta B - J/2 - \mathrm{D}_1$. In standard EPR experiments, the external oscillating magnetic field that induces the transitions is linearly polarized perpendicular to the static magnetic field, along the x axis for example. The transition probability P_{if} between two states $|i\rangle$ and $|f\rangle$ is proportional to the square of the matrix element $\langle f|g_{\perp}S_x|i\rangle$, which gives

$$P_{if} \propto \begin{pmatrix} 0 & 0 & 1 & 0 \\ 0 & 0 & 0 & 0 \\ 1 & 0 & 0 & 1 \\ 0 & 0 & 1 & 0 \end{pmatrix} \tag{14}$$

written in the order $\{|\varphi_1\rangle, |\varphi_2\rangle, |\varphi_3\rangle, |\varphi_4\rangle\}$. Because H_{pair} does not mix states of the triplet with the state of the singlet, EPR transitions [Eq. (14)] are only allowed within the triplet states between $|\varphi_1\rangle$ and $|\varphi_3\rangle$ and between $|\varphi_3\rangle$ and $|\varphi_4\rangle$. The isotropic exchange interaction J cannot be measured, and the EPR pair spectrum is only composed of two lines that are symmetrically placed around $g_{//}\beta B$ at energies $g_{//}\beta B \pm D$ with $D = D_1 + D_3$. These two transitions are indicated in Figure 3 for the $^{\text{even}}$Yb–$\mathrm{V_{Cd}}$–$^{\text{even}}$Yb pair center. Figure 4 shows the observed angular variations of the two transitions due to the $^{\text{even}}$Yb–$\mathrm{V_{Cd}}$–$^{\text{even}}$Yb pair center. The two transitions cross over at an angle of 53.68 degrees very close to the value of 54.44 degrees corresponding with a pure point dipole–dipole interaction between the two electronic spins. This provides confirmation that we can use a pure dipole–dipole expression for D_1, D_2, and D_3.

The situation is different when one ion (ion 1 for example) has a nuclear spin $I \neq 0$ (pairs of the type ^{171}Yb–$\mathrm{V_{Cd}}$–$^{\text{even}}$Yb and ^{173}Yb–$\mathrm{V_{Cd}}$–$^{\text{even}}$Yb). If

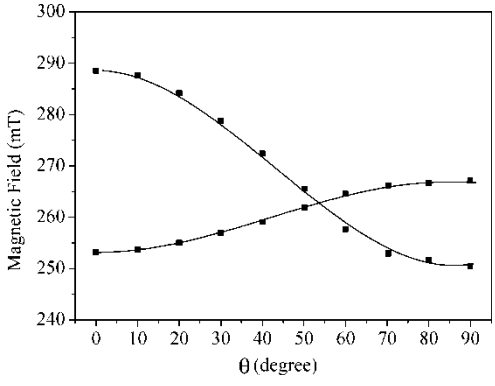

Figure 4. Experimental and calculated angular variations in the (ac) or (bc) crystallographic plane of the two EPR pair transitions of the ^{even}Yb–V_{Cd}–^{even}Yb pair center in $CsCdBr_3$.

M_I is the projection of the nuclear spin I of ion 1, the following basis set has to be considered

$$\left\{\left|-\frac{1}{2},-\frac{1}{2},M_I\right\rangle,\left|-\frac{1}{2},\frac{1}{2},M_I\right\rangle,\left|\frac{1}{2},-\frac{1}{2},M_I\right\rangle,\left|\frac{1}{2},\frac{1}{2},M_I\right\rangle,\ldots\right\}$$

with $-I \leq M_I \leq I$. The basis is composed of $4(2I+1)$ vectors. When we take into account the hyperfine interaction on spin 1, H_{pair} becomes

$$H_{pair} = H_1 + H_2 + H_{\text{int}} + A_{//}S_{Iz}I_z + \frac{A_\perp}{2}(S_{1+}I_{1-} + S_{1-}I_{1+}). \qquad (15)$$

The last part of the hyperfine interaction $A_\perp/2(S_{1+}I_{1-} + S_{1-}I_{1+})$, for a given M_I value, mixes the state $|-1/2,-1/2,M_I\rangle$ with the state $|1/2,-1/2,M_I-1\rangle$, the state $|-1/2,1/2,M_I\rangle$ with the state $|1/2,-1/2,M_I-1\rangle$, the state $|1/2,-1/2,M_I\rangle$ with the state $|-1/2,1/2,M_I+1\rangle$, and the state $|1/2,1/2,M_I\rangle$ with the state $|-1/2,1/2,M_I+1\rangle$. All these off-diagonal terms induce mixing between the electronic part of the wavefunctions and in particular between the electronic singlet and electronic triplet. EPR transitions thus become allowed between all these levels, and the isotropic exchange interaction can be then measured. We expect $4(2I+1)$ allowed transitions when one ytterbium isotope of a pair has a nuclear magnetic moment. Thus for the ^{171}Yb–V_{Cd}–^{even}Yb pairs, there are eight transitions, whereas for the ^{173}Yb–V_{Cd}–^{even}Yb pairs, there are 24 allowed transitions. The analytical expressions of the position of the resonance lines obtained by a perturbative treatment up to second order as well as their intensity are given in Ref. 3. The spin-Hamiltonian parameters of Eq. (15) are calculated and we find an exchange interaction $J = -48 \pm 6$ MHz. The g, A, and D parameters are given in Ref. 3. We

do not have to take into account pairs of the type $^{171}Yb-V_{Cd}-^{171}Yb$, $^{171}Yb-V_{Cd}-^{173}Yb$, and $^{173}Yb-V_{Cd}-^{173}Yb$, which are at low concentration compared with $^{171}Yb-V_{Cd}-^{even}Yb$, and $^{173}Yb-V_{Cd}-^{even}Yb$ pairs. The position and intensities of the most important lines are depicted as a stick diagram in Figure 3. In the case of $^{173}Yb-V_{Cd}-^{even}Yb$ pairs, eight very weak resonance lines in the 252–284 mT field range, are not shown.

The agreement between the calculated and experimental lines is excellent with a spread of 0.4% compared with the overall splittings.

CONCLUSIONS

In this paper, we have shown that EPR spectroscopy is an interesting spectroscopy for the study of the hyperfine structure of rare-earth ground-state levels and can thus be combined with hole burning spectroscopy for the complete determination of the hyperfine structure of an optical transition. Moreover, the study of EPR hyperfine structure often brings important information to the understanding of rare earth–rare earth interactions. Indeed, it can sometimes allow us to retrieve the isotropic exchange interaction, which is not possible with EPR spectra of pairs of identical rare-earth ions with no nuclear spin.

REFERENCES

1. Macfarlane, R.; Shelby, R. Coherent transient and hole burning spectroscopy of rare-earth ions in solids. In *Spectroscopy of Solids Containing Rare-Earth Ions*; Kaplyanskii, A. A., Macfarlane, R. (eds.).; Elsevier Science Publications: Amsterdam, 1987, 51–184.
2. Guillot-Noël, O.; Goldner, Ph.; Bettinelli, M.; Cavalli, E. Electron paramagnetic resonance study of multisite character of Yb^{3+} ions in $LuVO_4$ single crystals. *J. Phys. Condens. Matter* **2005**, *17*, 3061–3072.
3. Mehta, V.; Guillot-Noël, O.; Simons, D.; Gourier, D.; Goldner, Ph.; Pellé, F. EPR identification of coupled Yb^{3+} ion pairs in optically bistable compound $CsCdBr_3$:Yb. *J. Alloy. Compd.* **2001**, *323–324*, 308–311.
4. Guillot-Noël, O.; Goldner, Ph.; Higel, P.; Gourier, D.; A practical analysis of electron paramagnetic resonance spectra of rare-earth ion pairs. *J. Phys. Condens. Matter* **2004**, *16*, R1–R24.
5. Abragam, A.; Bleaney, B.; *Electron Paramagnetic Resonance of Transitions Ions*; Dover Publications: New York, 1986.
6. Böttger, T.; Thiel, C. W.; Sun, Y.; Cone, R. L. Optical decoherence and spectral diffusion at 1.5 μm in Er^{3+}:Y_2SiO_5 versus magnetic field, temperature, and Er^{3+} concentration. *Phys. Rev. B* **2006**, *73,* 075101-1-16.
7. Guillot-Noël, O.; Binet, L.; Gourier, D. General conditions for intrinsic optical bistability at the atomic and molecular scale: an effective spin-Hamiltonian approach. *Phys. Rev. B* **2002**, *65,* 245101-1-20.
8. Ohlsson, N.; Mohan, R. K.; Kröll, S. Quantum computer hardware based on rare-earth-ion-doped inorganic crystals. *Optics Commun.* **2002**, *201*, 71–77.